



University of Groningen

Advanced receivers for submillimeter and far infrared astronomy

Kooi, Jacob Willem

IMPORTANT NOTE: You are advised to consult the publisher's version (publisher's PDF) if you wish to cite from it. Please check the document version below.

Document Version

Publisher's PDF, also known as Version of record

Publication date:

2008

[Link to publication in University of Groningen/UMCG research database](#)

Citation for published version (APA):

Kooi, J. W. (2008). Advanced receivers for submillimeter and far infrared astronomy. s.n.

Copyright

Other than for strictly personal use, it is not permitted to download or to forward/distribute the text or part of it without the consent of the author(s) and/or copyright holder(s), unless the work is under an open content license (like Creative Commons).

Take-down policy

If you believe that this document breaches copyright please contact us providing details, and we will remove access to the work immediately and investigate your claim.

Downloaded from the University of Groningen/UMCG research database (Pure): <http://www.rug.nl/research/portal>. For technical reasons the number of authors shown on this cover page is limited to 10 maximum.



rijksuniversiteit
 groningen

Advanced Receivers for Submillimeter and Far Infrared Astronomy

Proefschrift

ter verkrijging van het doctoraat in de
Wiskunde en Natuurwetenschappen
aan de Rijksuniversiteit Groningen
op gezag van de
Rector Magnificus, dr. F. Zwarts,
in het openbaar te verdedigen op
maandag 22 december 2008
om 16:15 uur

door

Jacob Willem Kooi

geboren op 12 juli 1960
te Geldrop

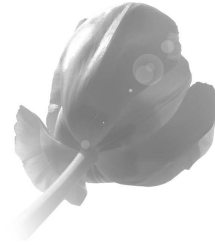
Promotores: Prof. dr. W. Wild
Prof. dr. ir. T.M. Klapwijk

Beoordelingscommissie: Prof. dr. R. F. Peletier
Prof. dr. M. W. M. de Graauw
Prof. dr. V. Belitsky

To my wife Helen

and my two sons

David and Andreas



Cover Front: *Caltech Submillimeter Observatory on top of Mauna Kea, Hawaii. Photograph was taken by the author during full moon on October 12, 2006, at 3 o'clock in the morning. Exposure time was 61s, f/5.6, and ISO 200 sensitivity. Projected in the foreground is a high altitude balloon heading for the stratosphere to carry out atmospheric and astrophysical observations.*

– Back: *The Herschel space observatory pointed at star forming regions in M33 (the pinwheel galaxy) in the constellation Triangulum. The distance from our “own” galaxy, the Milky Way, to M33 is approximately 3 million lights years. To avoid attenuation from water in the Earth atmosphere, follow up astrophysical observations may eventually be carried out by aircraft such as Sofia, at low precipitable water vapor sites in Antarctica, the Atacama desert in Chile (not shown), Mauna Kea in Hawaii, and by future space missions.*

Copyright © 2008 by J. W. Kooi.

Printed by: PrintPartners Ipskamp B.V., Enschede, The Netherlands.

Contents

1	Introduction	1
1.1	Submillimeter and far-infrared astronomy	1
1.1.1	Interstellar medium	3
1.1.2	Star formation	6
1.1.2.1	Molecular clouds	6
1.1.2.2	Spectral line surveys	8
1.1.3	Galaxies	9
1.1.4	Solar system	10
1.1.4.1	Planets	10
1.1.4.2	Comets	13
1.2	Coherent (heterodyne) detection	14
1.2.1	Challenges	14
1.2.2	Why high resolution spectroscopy	16
1.3	Contribution to the field of far-infrared astronomical instrumentation	17
1.3.1	Thesis outline	17
1.3.2	Impact on astronomy	18
2	Submillimeter detection and instrumental requirements	27
2.1	Introduction/Overview	27
2.2	Incoherent (direct) detection	29
2.2.1	Bolometers	30
2.2.2	TES	32
2.2.3	Photon fluctuation noise	32
2.2.4	Emissivity, optical efficiency, and sky noise	33
2.2.5	Background limited detection	34
2.2.5.1	Example 1: A 80 K space telescope	34
2.2.5.2	Example 2: A 4 K (cooled) space telescope	35
2.2.5.3	Example 3: A warm ground based telescope	35
2.3	Coherent (heterodyne) detection	35
2.3.1	Sensitivity of a heterodyne receiver	38
2.3.2	Conversion of NEP to system noise temperature	40
2.3.3	IF Bandwidth	42
2.3.4	RF Bandwidth	43
2.3.5	Instrument stability and baseline quality	43

2.3.6	Calibration	46
2.3.6.1	Two-load calibration	46
2.3.6.2	One-load calibration	48
2.4	Atmospheric transmission	49
2.5	Summary	52
3	Heterodyne receiver concepts	57
3.1	Mixing elements	57
3.1.1	Schottky-diodes	57
3.1.2	SIS tunnel junctions	59
3.1.3	Hot electron bolometer mixers	59
3.2	The single-ended Receiver	59
3.3	The switched-load (Dicke) receiver	61
3.4	The interferometer receiver	62
3.5	The balanced receiver	63
3.6	The correlation receiver	63
3.7	The sideband separating receiver	64
3.8	Summary	65
4	Fundamentals of SIS and HEB mixers	71
4.1	SIS mixers: Introduction	71
4.1.1	Photon-assisted quasiparticle tunneling	72
4.1.2	The Josephson effect	75
4.1.3	Network representation	76
4.1.4	Current in an SIS junction	77
4.1.5	Small-signal 3-port mixer model	81
4.1.6	Noise properties	83
4.1.7	SIS Mixer properties	84
4.1.7.1	RF reflection coefficient	84
4.1.7.2	IF output admittance and conversion gain	85
4.1.7.3	Calculated receiver performance	87
4.1.8	RF matching networks below the energy gap	87
4.1.9	Sensitivity to operating temperature	93
4.1.10	IF bandwidth	96
4.1.11	SIS mixer stability as a function of magnetic field	100
4.2	Electrodynamics and the non-local anomalous limit	103
4.2.1	Transmission line model	103
4.2.2	Plane waves in lossy dielectrics	104
4.2.3	Plane waves in good conductors	105
4.2.4	Surface impedance of normal metals	106
4.2.5	Surface impedance of superconductors	107
4.3	HEB mixers: Introduction	110
4.3.1	Electro-thermal Feedback and IF Standing Waves	115
4.3.2	Investigation of direct detection	118
4.3.2.1	HIFI	122
4.3.3	Effect on instrument calibration	123

4.3.4	Parametric stability	123
4.4	Summary	125
5	Quasi-optical mixers	137
5.1	Introduction	137
5.1.1	Waveguide Loss	137
5.1.2	Absorption loss above the superconducting energy gap	139
5.2	Physical implementation of a 850 GHz twin-slot mixer	142
5.3	Optics	143
5.4	Nb/AlN/NbTiN SIS junction with NbTiN wire layers	144
5.5	Performance	146
5.6	Astronomical observations	147
5.7	Summary	148
6	IF impedance and mixer gain of NbN hot-electron bolometers	153
6.1	Introduction	154
6.2	Theory	155
6.3	Experiment and calibration	158
6.4	IF impedance	160
6.5	Mixer conversion gain and the effect of electro-thermal feedback	162
6.6	Increasing the IF bandwidth of hot electron bolometers	165
6.7	Conclusion	167
7	A 275–425 GHz tunerless waveguide receiver based on AlN SIS technology	173
7.1	Introduction	174
7.2	Instrument design	175
7.2.1	Broad bandwidth waveguide-to-microstrip Transition	175
7.2.2	New set of SIS junctions	177
7.2.3	Nb/AlN _x -Al/Nb junction fabrication	178
7.2.4	Multiple Andreev Reflection (MAR)	180
7.2.5	Planar 4 – 8 GHz IF matching network, dc-break, bias Tee, and EMI filter	181
7.2.6	4 – 8 GHz low noise cryogenic amplifier	183
7.2.7	Cooled optics	183
7.3	Receiver performance	185
7.3.1	Fourier transform spectrometer measurements	185
7.3.2	Heterodyne results and discussion	185
7.3.3	IF response	190
7.3.4	Stability	191
7.3.5	Observations	192
7.4	Conclusion	194

8	Advanced receiver implementations	201
8.1	Introduction	201
8.2	Balanced mixer theory	202
8.2.1	The 180° balanced mixer	204
8.2.2	Amplitude noise immunity of a 180° balanced mixer	204
8.2.3	The 90° balanced mixer	206
8.2.4	Amplitude noise immunity of a 90° balanced mixer	207
8.3	Realization of 90° balanced-input receivers	208
8.3.1	Improved quadrature-hybrid waveguide coupler	209
8.3.2	Integrated IF and Wilkinson in-phase power combiner	211
8.3.3	SIS Junctions with integrated IF matching	214
8.3.4	Predicted performance	214
8.4	The correlation receiver	218
8.4.1	Introduction	218
8.4.2	Theory	218
8.4.2.1	Correlator back-end processor	220
8.4.2.2	AOS back-end processor	222
8.4.3	Observational analysis	222
8.4.4	Physical implementation	223
8.5	The sideband separating receiver	224
8.5.1	Introduction	224
8.5.2	Sideband separating mixer layout	225
8.5.3	Theory	226
8.5.4	SIS junction and waveguide transition simulations.	228
8.5.5	2SB computer simulations results	230
8.5.6	Integrated planar IF	231
8.5.7	Physical implementation	232
8.5.8	Measurement results	233
8.5.9	Atmospheric noise and the effect on 2SB and DSB receivers	235
8.6	Summary	237
9	Towards integrated array receivers	245
9.1	Introduction	245
9.2	SIS mixer fabrication on 1 μm thick Si_3N_4 membranes	246
9.2.1	Device fabrication	247
9.2.2	Measured performance	248
9.3	HEB mixers on ultra-thin silicon substrates	249
9.3.1	Introduction	249
9.3.2	Silicon-On-Insulator (SOI) morphology	251
9.3.3	SOI Processing	253
9.3.4	“Symmetric” SOI-based waveguide transition	253
9.3.5	“Asymmetric” SOI-based waveguide transition	255
9.4	Large format arrays based on SOI technology	257
9.4.1	Camera layout	259
9.4.2	LO power distribution	261
9.4.3	3 μm thick silicon splitblock waveguide transition	261

9.4.4	SIS junction design and predicted performance	264
9.4.5	Tolerance to misalignment and fabrication	267
9.4.6	Integrated IF	268
9.4.7	Fourier transform spectrometer (FTS) measurements	270
9.4.8	Heterodyne results	272
9.5	Summary	272
10	Stability of heterodyne receivers at terahertz frequencies	279
10.1	Introduction	280
10.2	Stability of small volume HEB mixers	282
10.2.1	Experimental setup	282
10.2.2	Continuum stability	284
10.2.3	Spectroscopic stability	286
10.3	Atmospheric and mechanical receiver stability	288
10.3.1	LO path length loss	289
10.3.2	Standing waves in the LO – mixer path	289
10.3.3	Estimate of allowed LO power fluctuations	291
10.3.4	Sensitivity to atmospheric turbulence	292
10.3.5	Sensitivity to mechanical fluctuations	293
10.4	Experimental validation	294
10.5	Conclusion	295
A	The Allan variance method	301
A.1	Introduction	301
A.2	Theoretical considerations	302
A.3	Total Power Allan variance	305
A.4	Spectroscopic Allan variance	306
A.5	Improvement of spectroscopic over total power Allan variance	307
B	Transmission properties of Zitex	311
B.1	Introduction	311
B.2	Zitex G104, G106, G108, G110, G115, & A155	312
B.3	Multiple Layers	313
B.4	Temperature Variation	314
B.5	Refractive Index	315
B.6	Thermal Conductivity	315
C	AR coated HDPE windows	319
C.1	Introduction	319
C.2	Antireflection coating	321
C.3	Multi-layer antireflection coating	321
	Nederlandse Samenvatting	327
	Acknowledgements	333

List of publications

337